Stellar astrophysics illustrated by the GAIA DR2 HR diagram

Haochuan Li

Abstract: GAIA is a telescope providing astrometric and photometric data with unprecedented quantity and quality. A lot of interesting features are revealed on the HR diagram with the help of its 2nd data release. This article is going to show some of these features and provide relevant discussions to the maximum extent I can.

1. Introduction of GAIA telescope

GAIA is a telescope launched on Dec.19, 2013 by European Space Agency. It is an ambitious telescope providing astrometric and photometric measurements of a large quantity of stars, which are the cornerstone for astronomy. Table 1 records the number of stars in GAIA Data Release 2 samples. Compared to previous sky surveys, like SEGUE-2 and APOGEE which obtain spectra of around 140 thousand stars (Constance et al, 2009), the number of stars offered by GAIA DR2 alone wins by orders of magnitude. In addition to the quantity, the quality is also high. Take parallax as an example, GAIA measures distance with a precision of at least 1% for some 10 million stars and at least 10% for some 100 million stars (Gaia collaboration, A.G.A.Brown et al, 2018). Finally, the measurements are conducted for several dozen times in GAIA's entire mission which pictures the evolution of our interested physical quantities with time. Such multi-measurement is the basis of plots like Fig.20 in this article.

The high quantity and quality of both astrometric and photometric data directly lead us to a famous diagram in astronomy: the HR diagram. With the numerous sample offered by the 2nd data release of GAIA (Referred to as GAIA DR2 later) in April 2018, lots of interesting features shows on the HR diagram involving both the general HR diagram and the HR diagram of some specific types of objects, with some proving past theories and others being novel.

In this article, I am going to present some features on the HR diagram with theoretical discussions of the vast related field of astrophysics to the maximum of my awareness. We should keep in mind that novel features often indicate a new area of astrophysics and potential modification to our current theory.

Table 1. Number of sources of a given type or the number for which a given data product is available in *Gaia* DR2.

Data product or source type	Number of sources
Total	1 692 919 135
5-parameter astrometry	1 331 909 727
2-parameter astrometry	361 009 408
ICRF3 prototype sources	2820
Gaia-CRF2 sources	556 869
G-band	1 692 919 135
G_{BP}-band	1 381 964 755
G_{RP}-band	1 383 551 713
Radial velocity	7 224 631
Classified as variable	550 737
Variable type estimated	363 969
Detailed characterisation of light curve	390 529
Effective temperature T_{eff}	161 497 595
Extinction A_G	87 733 672
Colour excess $E(G_{BP} - G_{RP})$	87 733 672
Radius	76 956 778
Luminosity	76 956 778
SSO epoch astrometry and photometry	14 099

Tabel 1: Gaia's sample size shown as Tabel 1 in Gaia collaboration A.G.A.Brown et al, 2018

2. Sectional views of the HR diagram

In August 2018, Gaia Collaboration, C. Babusiaux et al, 2018 presented a detailed view of the newest GAIA DR2 HR diagram shown as Fig.1 here. Both figures in Fig.1 subject to parallax and flux precision cuts that parallax error < 10%, R and B band flux error <5%, G band flux error <2%, and extra cuts to avoid the influence of nearby objects (namely $1.0+0.015(B-R)^2 <$ phot_bp_rp_excess_factor$< 1.3 + 0.06\ (B-R)^2$). According to the author's own words, "many fine structures are present". This section is going to present some detailed views of different sections of the GAIA DR2 HR diagram.

A special note: the main sequence is not going to be discussed until Section 3, because it is much more interesting when we observe clusters.

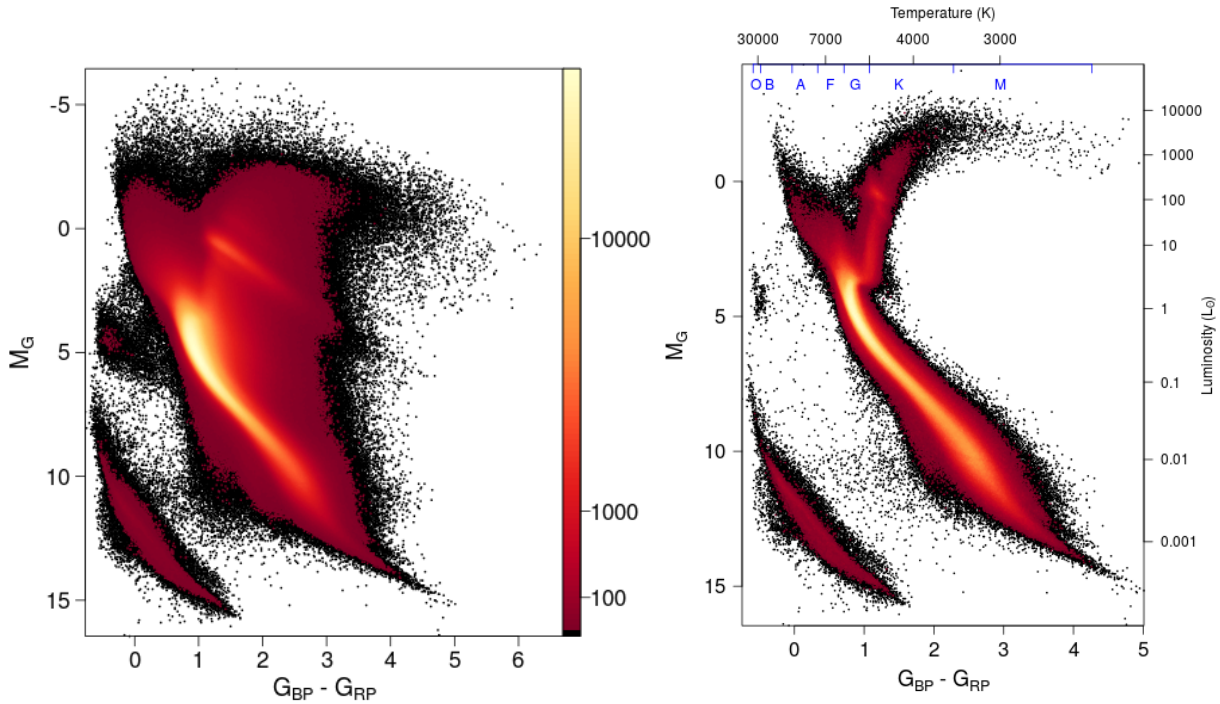

Fig.1 Left: Full GAIA DR2 HR diagram obtained from GAIA DR2 shown as Fig.5 in Gaia Collaboration, C. Babusiaux et al (2018). Right: GAIA DR2 HR diagram for low extinction sources (E(B-V)<0.015) shown as Fig.6 in Gaia Collaboration, C. Babusiaux et al (2018)

2.1 Brown Dwarf

For Main Sequence stars, the color shift to the red as stellar mass and T_{eff} go down. However, for brown dwarfs, it is first observed long ago that the infrared J-K color shift back to the blue when mass goes below a certain threshold. Such phenomenon is called the "L/T transfer" as the shifting point corresponds to the transition from L type brown dwarf to T type. Around the beginning of the 21st century, a few astronomers, including Ackerman and Marley (2001), Marley et al (2002) etc, argued that the migration and disruption of condensate clouds deep in the photosphere is a primary cause for the color shift. According to these papers, the height of water, silicon or iron clouds decreases with brown dwarf type changing from L to T and finally sinks "into" the star. The flux origination therefore gradually moves from below the clouds to above the clouds, causing difference in absorption and therefore changing color patterns. Besides the location, chemical changes also play a role, for example the J-K color "turning point" corresponds to K I atoms being transferred into KCl moleculars, and there are also other molecular forming patterns like Na I -> Na_2S. Li I -> LiOH/LiCl (Lodders, 1999), etc. Previously, the most successful model is the BT-Settl model illustrated by Allard. et al (2012a). The model is plotted together with other models shown as Fig.2 here, and we can clearly see that the BT-Settl model is the only one that could explain stars with all T_{eff}.

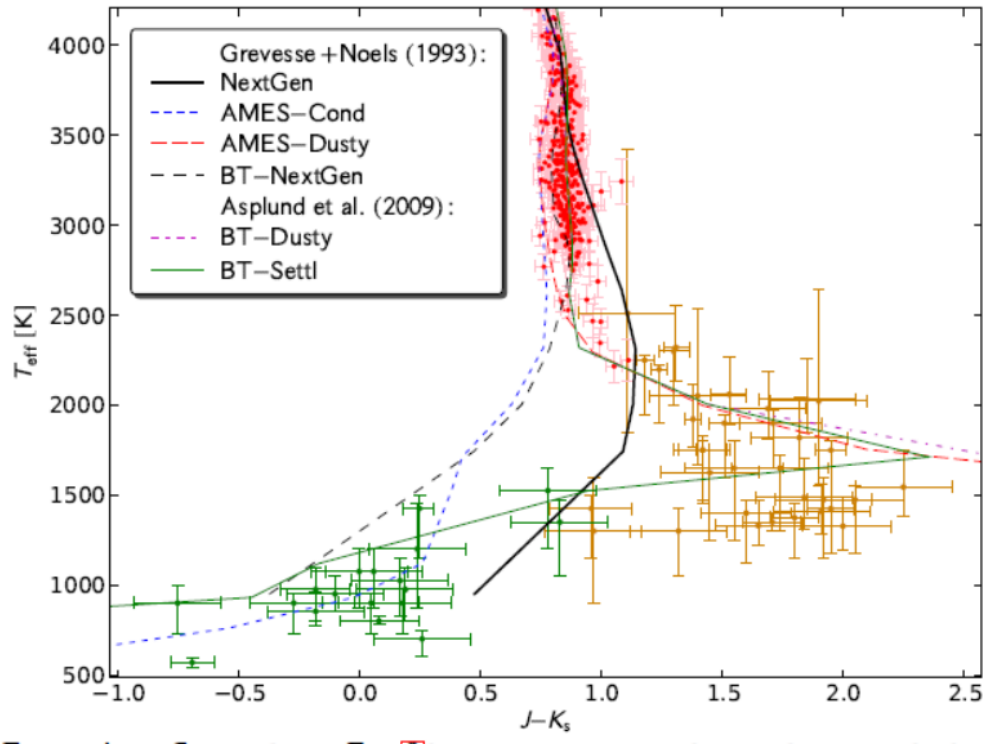

Fig.2 Comparison of different models of brown dwarfs and low mass stars shown as Fig.3 in Allard et al (2012)

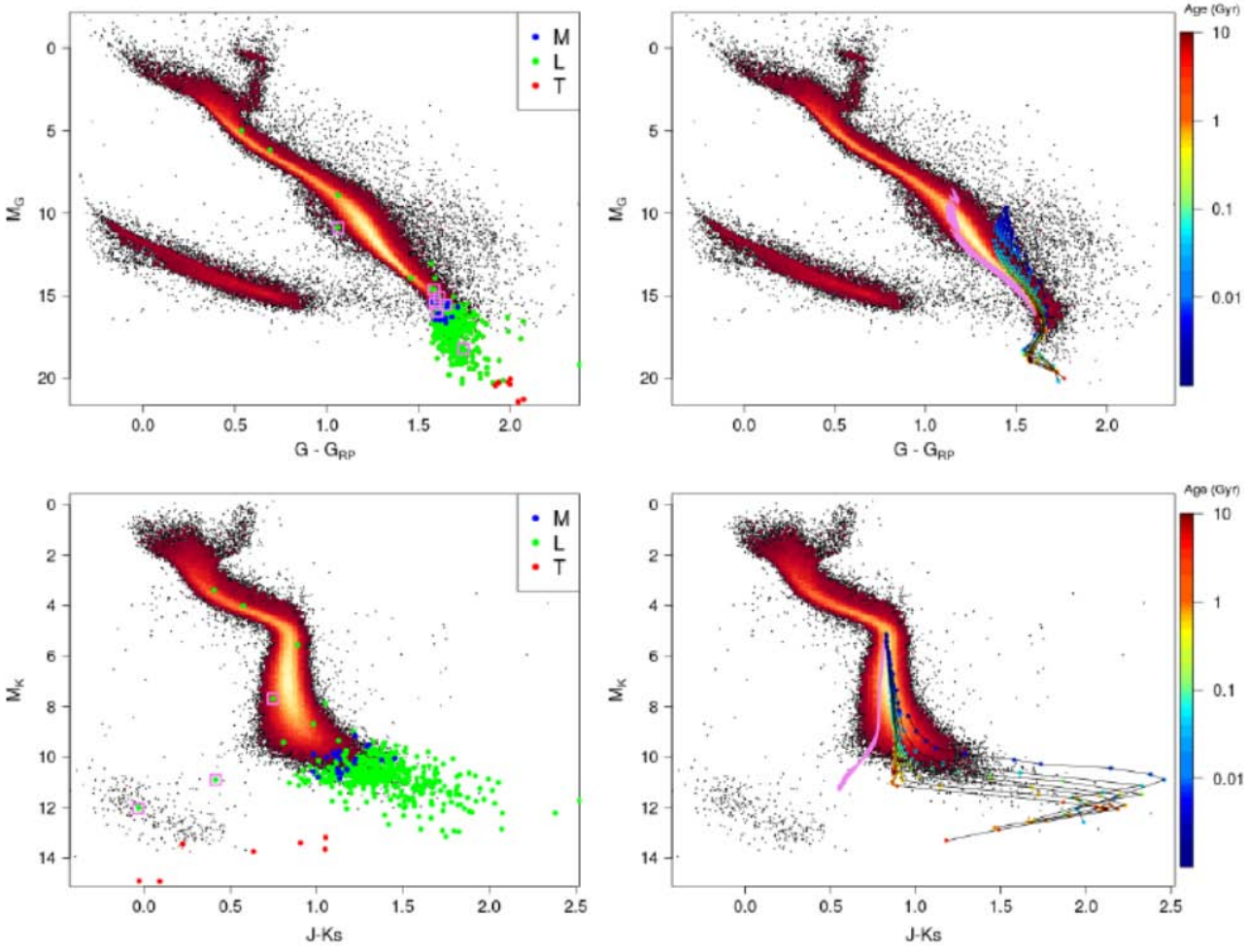

Fig.3 Locations of brown dwarfs and the BT-Settl tracks on the HR diagram shown as Fig.9 in Gaia Collaboration, C. Babusiaux et al (2018)

With GAIA DR2, the number of observed brown dwarfs with parallax error smaller than 10% rises several times to around 470 according to Gaia Collaboration, C. Babusiaux et al (2018). The authors plotted them on the HR diagram shown as Fig.3 here. The upper-left panel shows the locations of brown dwarfs on top of the HR diagram of solar neighborhood (distance<100pc) stars. The upper-right panel shows the BT-Settl tracks calculated according to GAIA passbands. The two lower panels are the same figures with different brightness and color indicators. In these plots, G_{BP} is never used for brown dwarfs because of the poor quality for such faint objects.

It is exciting to see that the actual data points distribute along the BT-Settl tracks with the clear infrared color turning pattern. The study of brown dwarf atmosphere is still not complete, but at least GAIA's observation gives a strong proof to previous model whose precision adds a lot to the persuasiveness.

2.2 Giant branch

Aside from widely understood Red Clump (RC), horizontal branch and Asymptotic Giant Branch (AGB), giant branch in the HR diagram contains other features. The most interesting ones are the Secondary Red Clump (SRC) and the Vertical Red Clump (VRC) which are actually one vertical strip left of RC.

The change in core degeneracy condition is crucial to the formation of this strip. To generate temperature for Helium burning, the lower the mass of the original star, the more the core has to contract. For low mass stars, the contraction is so strong that the electrons are degenerate, which is opposite to high mass star cores. In 1999, Girardi et al (1999) predicted the change of core mass, surface luminosity and temperature changing trend considering the difference core degeneracy. Their plot is shown as Fig.4 here. We can see that core mass remains constant for low mass stars with degenerate cores and drops at the threshold of core degeneracy removal, after which it increases linearly against stellar mass. The similar drop happens on luminosity, too. The temperature on the contrary, does not change too much for high mass stars. This is why we expect a vertical strip.

Fig.5 shows the GAIA's giant branch of Fig.1 right panel. All the interesting structures are labeled in blue letters. We can see the presence of a vertical strip which forms the VRC and SRC, which is again an observational proof to the theory.

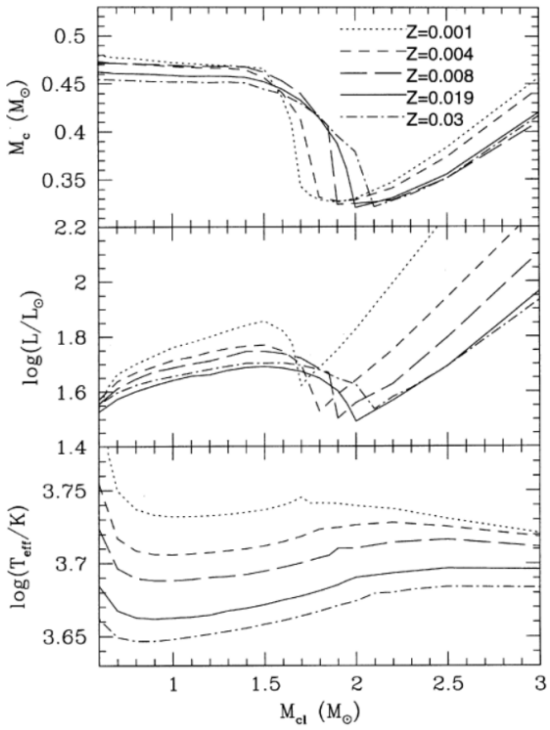

Fig.4 The behavior of core mass, luminosity and effective temperature of Helium burning giants shown as Fig.1 in Girardi (1999)

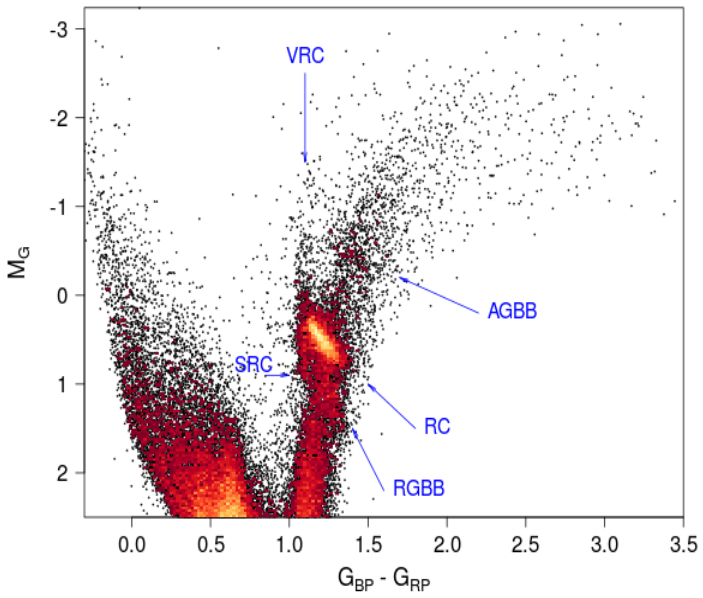

Fig.5 Giant branch of the HR diagram shown as Fig.11 in Gaia Collaboration, C. Babusiaux et al (2018)

2.3 White Dwarfs

Fig.6 here presents the detailed view of GAIA DR2 white dwarf sequence with parallax error < 20%. Again, there are some fine structures discussed in the next few paragraphs.

First, there are two obvious concentrations marked A and B in Fig.6 which merge at blue and red end and separate in the middle. People have also overplotted some cooling tracks (Bergeron et al 2011, Tremblay et al 2011) on the HR diagrams and color-color diagrams which are shown as Fig.7 here. Previously Kleinman et al. (2013) have examined SDSS DR7 catalogue and plotted a histogram of white dwarfs in it (Fig.8), which shows a concentration in the number distribution of white dwarfs between $0.5M_{sun}$~$0.8M_{sun}$ with a peak at $0.6M_{sun}$. In GAIA result (Fig.7), all three panels show a clear concentration along the magnet line representing the $0.6M_{sun}$ Hydrogen white dwarf cooling track (corresponding to concentration A in Fig.6), which is consistent with SDSS DR7.

An unexpected trend in Fig.7 upper panel is that concentration B seems to follow the green line representing $0.8M_{sun}$ Hydrogen white dwarf track around the maximum separation of A and B. To study this trend, authors of Gaia Collaboration, C. Babusiaux et al (2018) tried to plot the color-color magnitude of the same sample as Fig.7 upper panel as is shown in Fig.7 middle panel. Moreover, they tried to employ SDSS magnitudes and calculate absolute magnitude based on GAIA DR2 parallaxes, and plot the M_u against u-g color HR diagram shown as Fig.7 lower panel. Both show concentration on the two $0.6M_{sun}$ tracks as expected, and the lower panel involving SDSS magnitudes show a much bigger separation between concentrations A and B. There are some stars on the green line in the lower panel, but it is not quite obvious probably because of the faintness of the stars and the photometry limit of SDSS. In this way, the unexpected trend may be simply caused by the low resolution of Fig.7 upper panel.

Aside from concentrations A and B, it may be noticed that there is another concentration labeled Q which is much less obvious and lies around B-P=-0.2, M_G=13. Besides that, if we compare Fig.6 and Fig.7, we may find that the red end of concentration departs from the cooling tracks towards the red end, for example, the point B-R=1.5, M_G=15 is roughly on the concentration but clearly off the cooling tracks. These are newly observed features, and the detailed mechanisms are still unknown.

Finally, people examined the locations of different types of white dwarfs and compared the result of GAIA photometry and SDSS photometry, and the results show perfect agreement as shown in Fig.9 here. DA white dwarfs definitely take up the most space on the HR diagram, they are almost everywhere on the white dwarf sequence. DQ, DZ, DC white dwarfs all prefer the red end and low luminosity part of the white dwarf sequence, while the quite low-population DO white dwarfs prefer the blue end. DB white dwarfs tend to occupy the middle area.

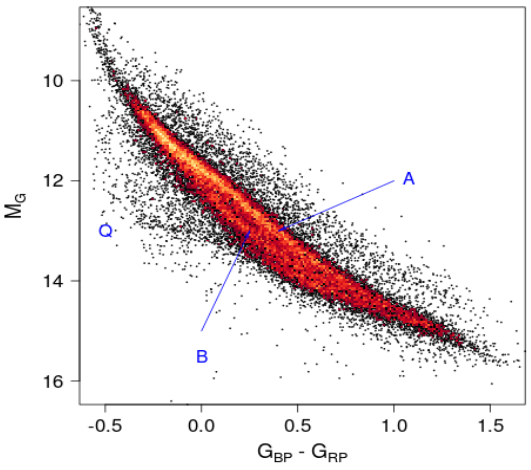

Fig.6 White dwarfs with parallax error < 20% shown as Fig.14 in Gaia Collaboration, C. Babusiaux et al (2018)

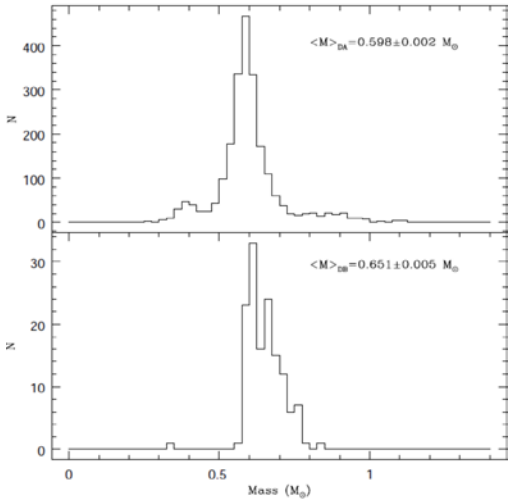

Fig.8 Histogram of SDSS DR7 white dwarfs. Samples are restricted to S/N≥15 and T_{eff}>13000/16000 K for DA/DB white dwarfs respectively.

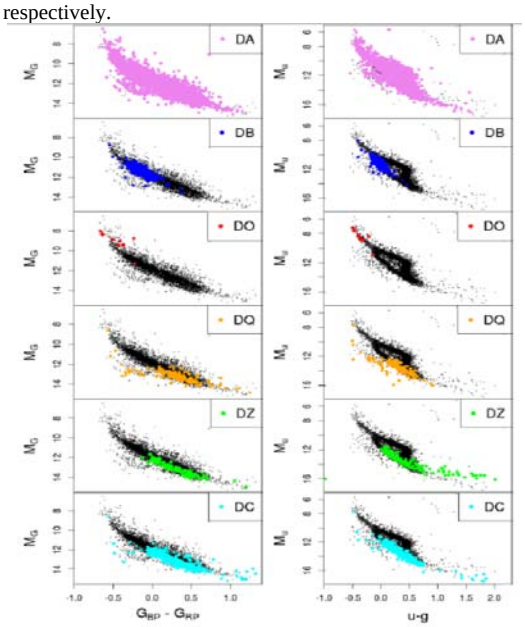

Fig. 16. SDSS white dwarfs per spectral type (DA: hydrogen; DB: neutral helium; DO: ionised helium; DQ: carbon; DZ: metal rich; and DC: no strong lines). panel a): *Gaia* photometry, panel b): SDSS photometry.

Fig.9 Comparison of locations of different types of white dwarfs between GAIA and SDSS photometry shown as Fig.17 in Gaia Collaboration, C. Babusiaux et al (2018)

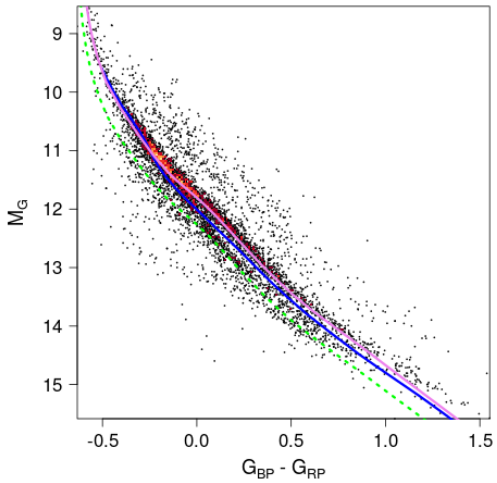

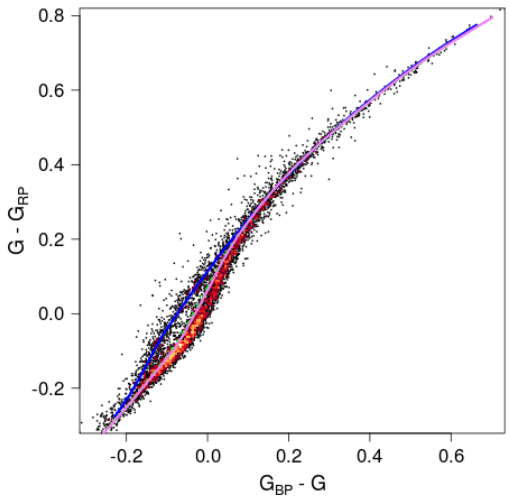

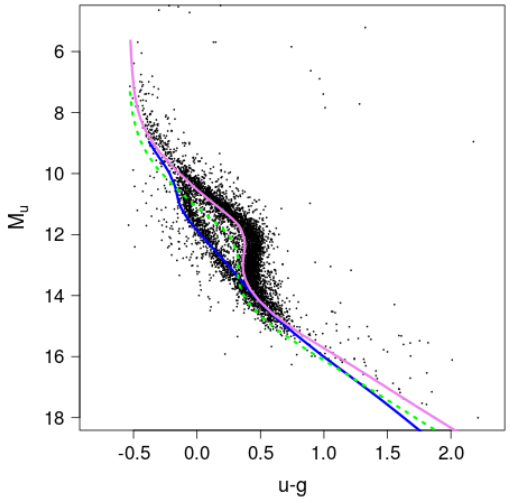

Fig.7 HR and color-color diagram of white dwarf sequence with evolutionary tracks shown as Fig.15 in Gaia Collaboration, C. Babusiaux et al (2018). Upper: HR diagram with data from GAIA DR2 with precision of parallax error < 5%. Middle: color-color diagram sharing the same data with left panel. Lower: HR diagram with SDSS color and magnitude which is converted to absolute magnitude using GAIA DR2 parallaxes. In all three panels, magnet, blue, green lines represent 0.6M_{sun} Hydrogen, 0.6M_{sun} Helium, 0.8M_{sun} Hydrogen white dwarf cooling tracks respectively

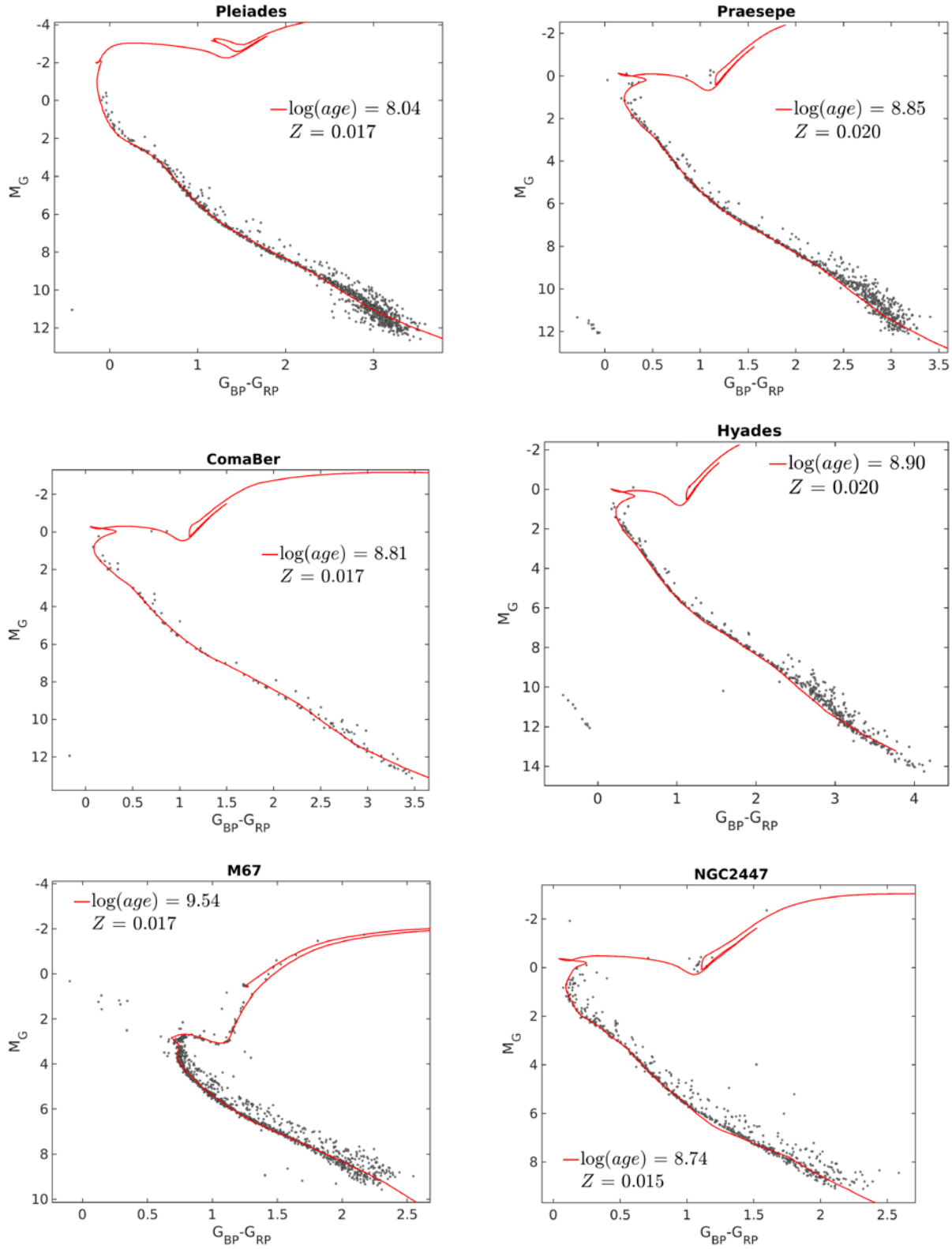

Fig.10 The HR diagram of some open clusters selected from Fig.19 in Gaia Collaboration, C. Babusiaux et al (2018)

3. Clusters on the HR diagram

Clusters are benchmarks of stellar astrophysics because they uniquely offer huge groups of stars sharing common properties. Open clusters hold stars sharing almost the same age and chemical compositions because of the identical origins and therefore illustrate isochrones of stellar evolution. Globular clusters on the other hand, were created from the primary nebulous gas soon after the formation of the Milky Way, therefore they have low mass, poor metallicity and trace the early chemical evolution of our Galaxy and the properties of low-mass stars. In the following paragraphs I will present features of the HR diagram of clusters based on GAIA DR2.

Fig.10 shows the HR diagram of some open clusters with red lines representing the newest accepted PARSEC-COLIBRI isochrones (Paola et al, 2017). Unlike Fig.1, the main sequence strips are very thin and concentrated along the red line with additional strips of constant ~0.75mag right above it. Considering that the magnitude difference between one star and a binary system sharing the same magnitude for both stars is $2.5 \lg 2 = 0.753$mag, the “additional strips” actually reflects the influence of binary systems.

The thin main sequence strips prove the existence of a strong relationship between the age, color, and luminosity, while current theory may be good but not perfect. The PARSEC isochrones shown as red line generally fits the main sequence strip well, but if we look carefully, there is a discrepancy at around M_G=10 for quite some clusters, which indicates some discrepancies between theory and observations and therefore potential improvement of the theory.

As for globular clusters, the most interesting feature is the diversity of horizontal branch (HB). Previously, Mucciarelli et al (2016) have found that Na-rich globular clusters tend to have blue HBs while Na-poor ones prefer red HBs. Since [Na/H] is often used to distinguish first- and second-generation stars, this indicates that blue HB globular clusters have more second-generation stars, which makes sense because there should be more early-type stars in second-generation stars nowadays and that should lead to stronger blue HB.

However, when we look at Fig.11 which shows the GAIA DR2 diagram of four globular clusters with different [Fe/H], the trend is exactly the opposite against that of [Na/H].This is a phenomenon that puzzles me a lot. Probably for such heavy metals, not all first generation stars can generate them, but it is still not enough to explain the exactly opposite behavior.

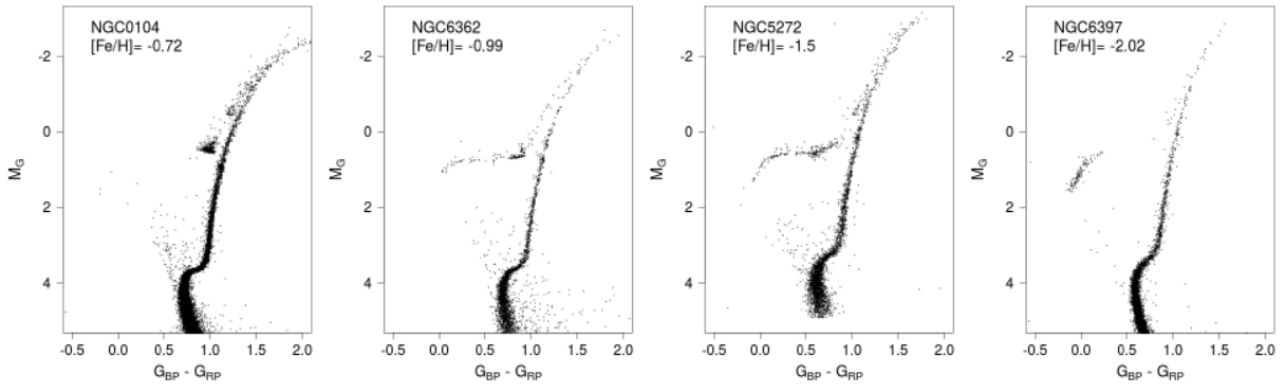

Fig.11 The HR diagram of four different globular clusters shown as Fig.11 in Gaia Collaboration, C. Babusiaux et al (2018)

4. Variable stars on the HR diagram

The concept of “variable star” only refers to the variability of luminosity. There are tons of different mechanisms leading to the variability, therefore variable star is an important field in astrophysics involving physics across the field. As an example, Fig.12 shows the most up-to-date classification tree of variable stars which is Fig.1 from Gaia collaboration, L.Eyer et al (2018).With GAIA DR2, it is possible to study currently observed variable stars in details. This section shows the views of variable stars with the help of HR diagram including their locations, fractions and motion tracks on the HR diagram.

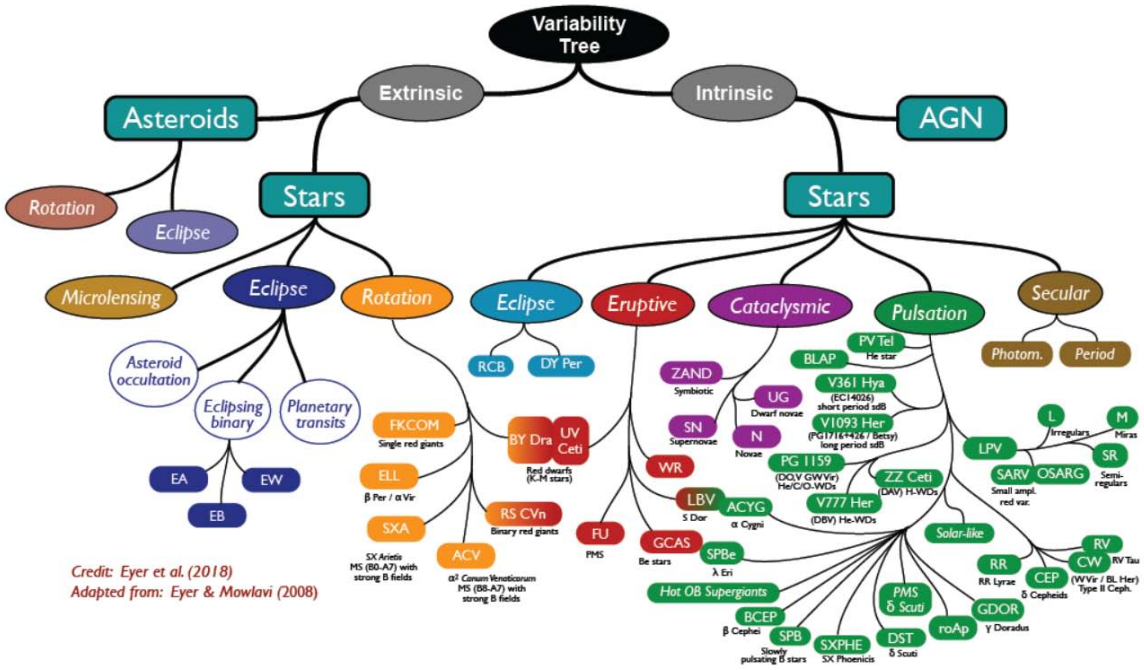

Fig.12 Variable tree as presented by Fig.1 from Gaia collaboration, L.Eyer et al, 2018

4.1 Static view: Locations and fraction of variables

Fig.13-16 show the locations of different types of variable stars. The detailed meanings of the names of all classifications can be found in Section 2 of Gaia collaboration, L.Eyre et al (2018). Again, the plots show a lot of features. Some of them are discussed below.

Fig.13 shows that ZZ Ceti stars seem to distribute as groups rather than lines along the white dwarf branch on the HR diagrams, which is probably a phenomenon whose mechanisms are still not understood. Fig.14 shows that the density of rotation-induced main sequence is a little lower around B-R=0.4 which is roughly the transition point of convective to radiative envelop. Moreover, reflection binary class is located almost all below the main sequence, implying that white dwarfs are better at reflecting the light from their companions. Fig.15 shows that eclipsing stars are almost everywhere through the main sequence strip and the giant star region. Interestingly, around B-R=0.5 and M_G=4, there is a concentration which is interpreted by the authors as white dwarfs with main sequence companion. Fig.16 shows a clear absence of eruptive variables around the blue end of main sequence strip. Such absence is so obvious that it even divides the eruptive variables into two groups on the HR diagram. Fig.17 shows that cataclysmic stars locate between main sequence and white dwarf branches, and even more near the location of ZZ Ceti stars, etc.

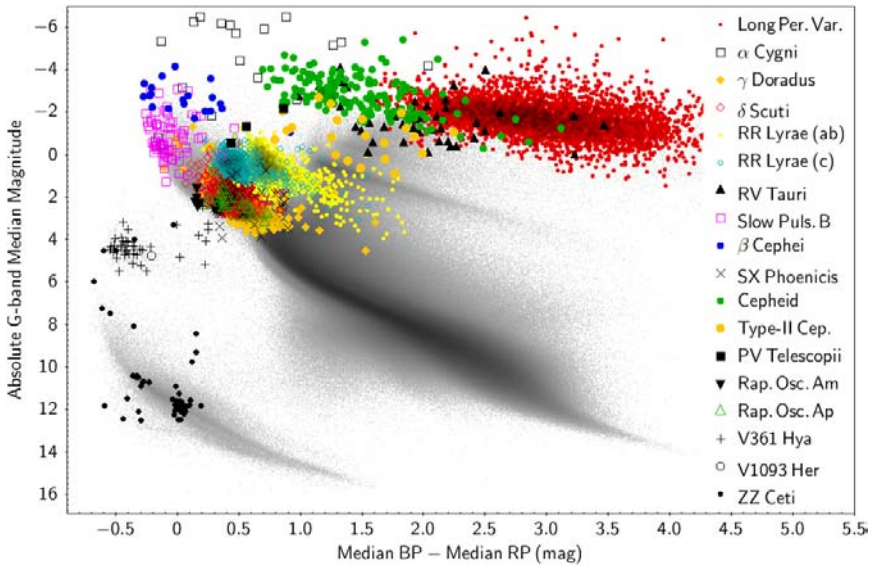

Fig.13 Pulsating variable stars retrieved from published catalogues on the HR diagram

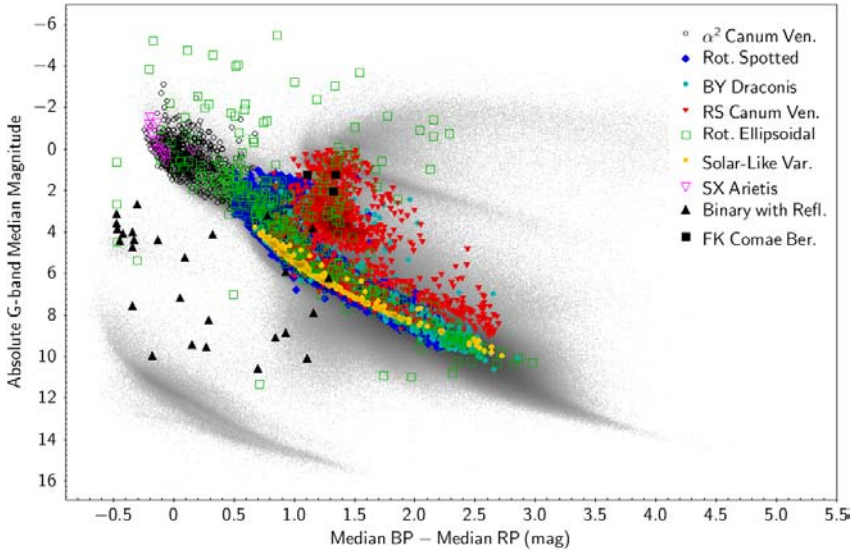

Fig.14 Rotational-induced variable stars retrieved from published catalogues on the HR diagram

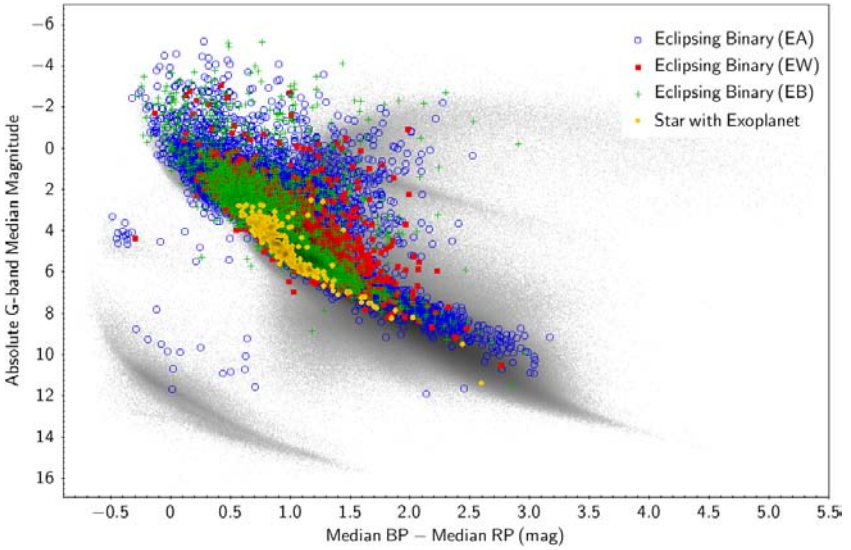

Fig.15 Eclipsing binaries retrieved from published catalogues on the HR diagram

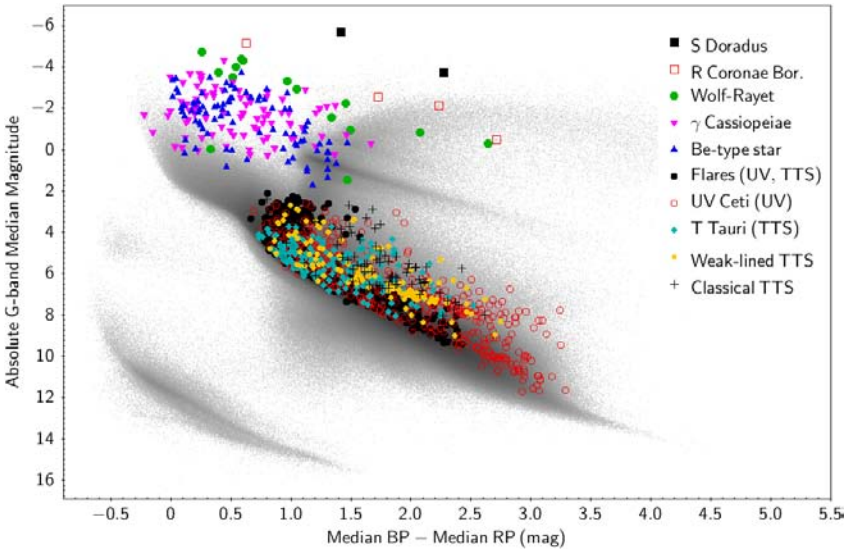

Fig.16 Eruptive variable stars retrieved from published catalogues on the HR diagram

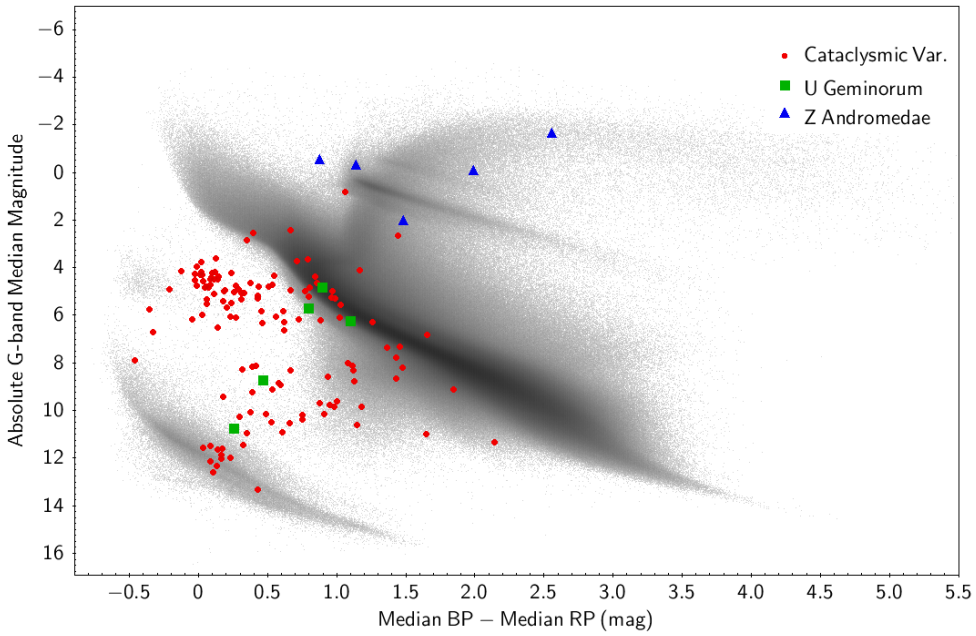

Fig.17 Cataclysmic variable stars retrieved from published catalogues on the HR diagram

Besides the locations of variables, fraction of variables is also studied. With a precision of maximum 5% error on parallax, 5% error on R and B band magnitude, 2% error on G band magnitude and |b|>5 deg to avoid extinction effect where b is the galactic latitude, the authors of Gaia collaboration, L.Eyre et al (2018) plotted the GAIA DR2 plotted high-resolution map of the variable fraction in the HR diagram shown as Fig.18 here. From this plot, we can see the strong preference of reddest and brightest giants for high fractions, the obvious classical instability strip on the main sequence strip although the fraction is not as high as ~1.0, and the increase of fraction with brightness for the same color within main sequence stars etc. Moreover, the region around B-R=-0.4, G=4 is almost filled with variable stars including ZZ Ceti stars (Fig.13), Binary with reflection component in the light curves (Fig.14) and cataclysmic variables (Fig.17). This might be an explanation for the concentration of stars here, and a lot of stars in this region might be unresolved binary systems involving white dwarfs.

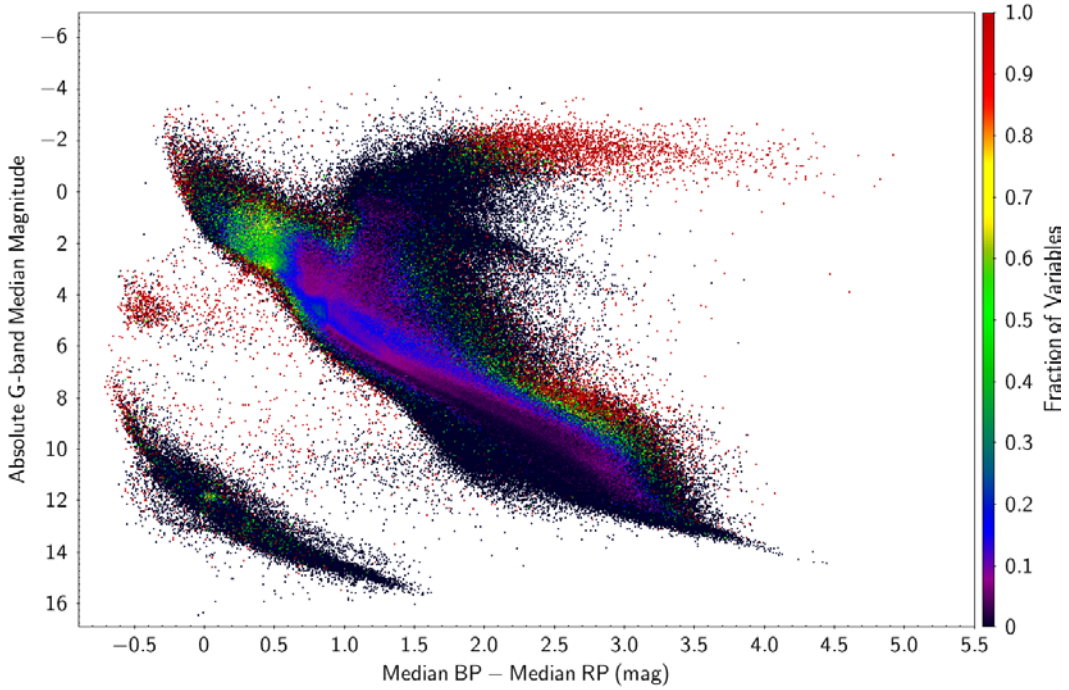

Fig.18 Variability fraction shown as Fig.6 in Gaia collaboration, L.Eyre et al (2018)

4.2 Variability amplitudes

Fig.19 shows the G band absolute magnitude variety amplitude showing some places preferable for large amplitudes, such as the red ends of giants and main sequence, the space between the white dwarf and main sequence strips, the ZZ Ceti group in the White Dwarf sequence, while the highest amplitude (>0.1 mag) seem to present all over the plot despite the non-uniform distribution. We may also see that the classical instability strip is not the leader in variability amplitude at all.

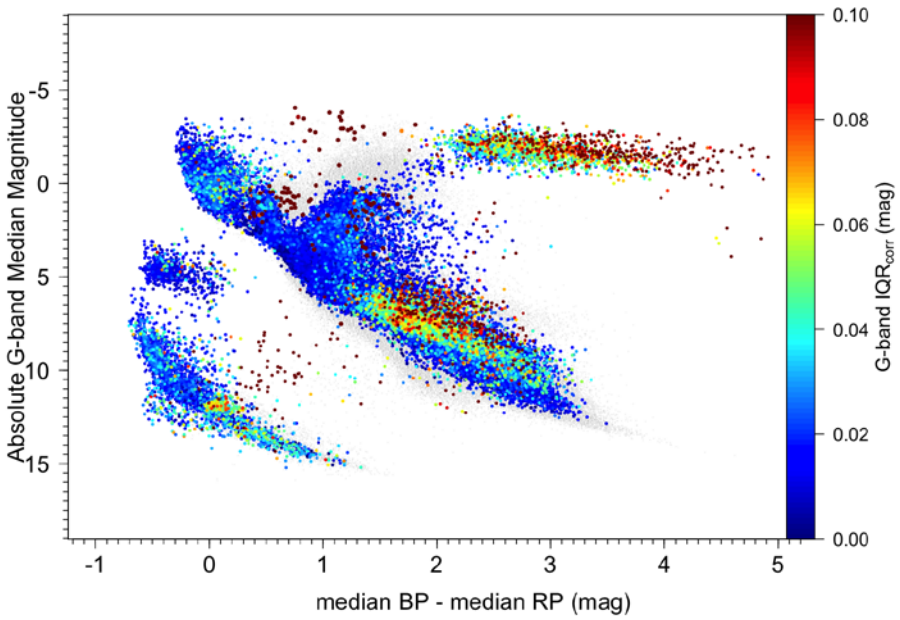

Fig.19 Variability amplitude on the HR diagram shown as Fig.7 in Gaia collaboration, L.Eyre et al (2018)

4.3 Motion tracks of variable stars on the HR diagram

Astrometric and photometric properties of stars are measured quasi-simultaneously for an average of several dozen times in GAIA's entire mission, therefore GAIA is particularly suitable for producing motion tracks on the HR diagrams. Fig.20 here visualizes these tracks for a subset of variables. Although the lines look a bit messy, we can easily separate this figure into several parts according to their shapes as discussed in the next paragraph.

Stars in the upper-right part, including Long Period Variables, Cepheids (both Classical and Type-II) and RR Lyare stars, are bluer when brighter and redder when dimmer. This is the characteristics of κ-mechanism which means that opacity and temperature increase/decrease together. Starting with high temperature with high opacity, heat accumulates and finally pushes matter outwards, the surface would cool because of expansion and the color reddens. The cooling decreases opacity and allows more radiation to penetrate the star which increases the observed luminosity, and vice versa. On the contrary, eruptive stars like Cassiopeia stars shown here are redder when they are brighter and that is probably caused by the extra extinction during their eruptive phase. The eclipsing binary systems in the middle part have tracks with much deeper slopes. This is not surprising because it is common that the two stars in a binary system have similar mass so the color won't change much, but the luminosity can change significantly by eclipsing. Since this is extrinsic cause, there should literarily be no universal track patterns for them. Finally, the cataclysmic variables at the bottom of the figure have remarkably large changes in color which is probably caused by the mass transfer from donor star.

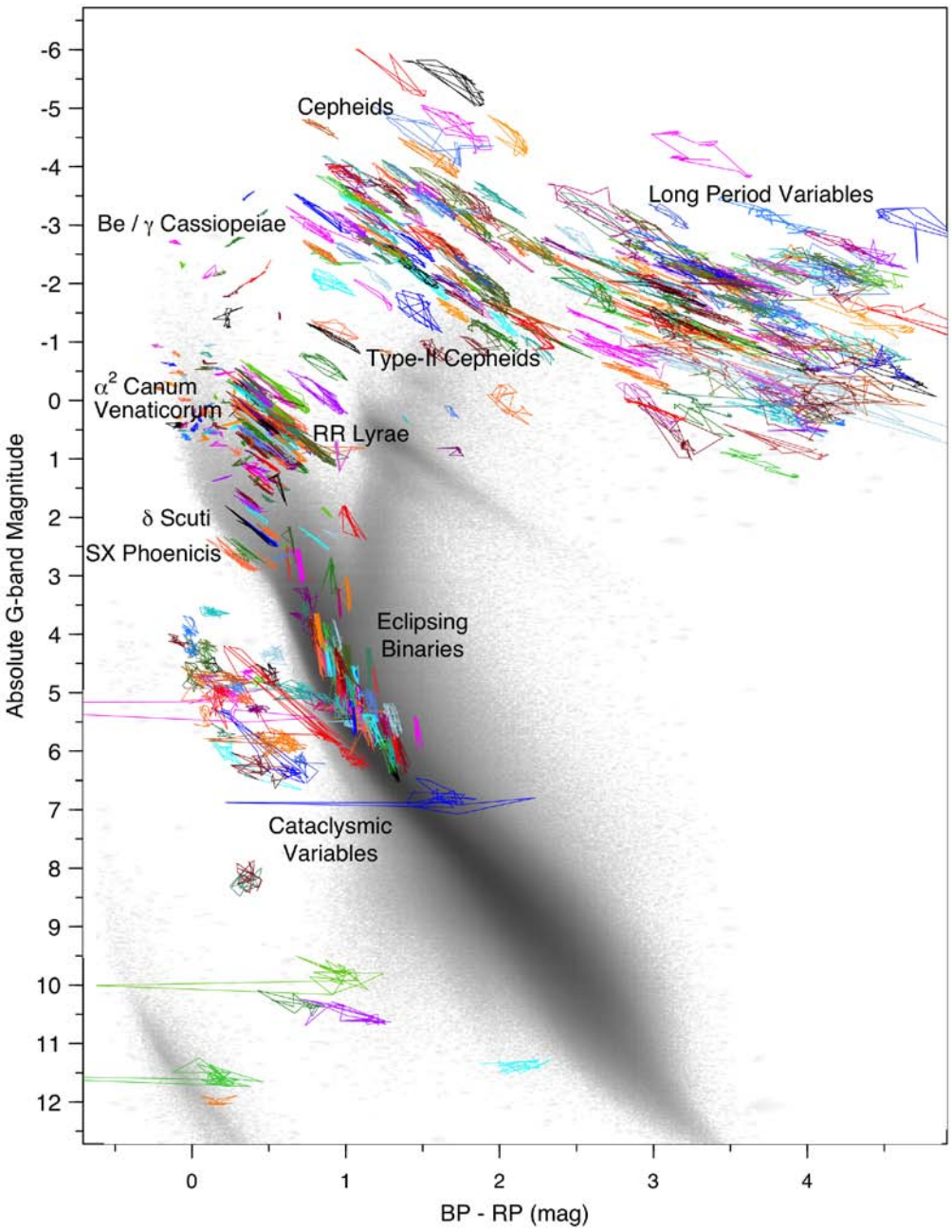

Fig.20 Motions of variable stars on the HR diagram shown as Fig.11 in Gaia collaboration, L.Eyre et al (2018)

5. Discussions and prospects

Near the end of the paper, I would like to present some of my own discussions to GAIA and astrophysics.

First of all, this paper only covers a small fraction of what GAIA will help us on stellar astrophysics. Take variable stars as an example, when GAIA mission was first proposed, Eyer and Cuypers (2000) predicted that about 18 million variable stars and about 5 million "classic" periodic variables will be observed among the total 1 billion stars. This is far beyond the sample size shown in this paper. Beyond variable stars, according to GAIA's official website (https://www.cosmos.esa.int/web/gaia/release), GAIA DR3 and DR4 will have non-single star catalogue, full set of astrometric and photometric data including radial velocities, an exo-planet list, etc. The prospect of stellar astrophysics is beyond measure.

If we look at the bigger picture, GAIA is also very helpful in areas other than stellar astrophysics. A very important example that we should be aware of is the Galactic dynamics which almost has to be studied because of

GAIA's huge sample size. For example, Benett and Bovy (2018) found vertical counts asymmetry for the stars within a 250pc radius vertical cylinder centered at our Sun, and their asymmetry plot is shown as Fig.21. Antoja et al (2018) found spiral patterns in number counts, v_r and v_ϕ distribution in z-v_z phase space in a sample of stars within 200pc from the Sun shown as Fig.22 here. It is certain that GAIA really reveals tons of secrets in various aspects of astrophysics that are yet to be explained.

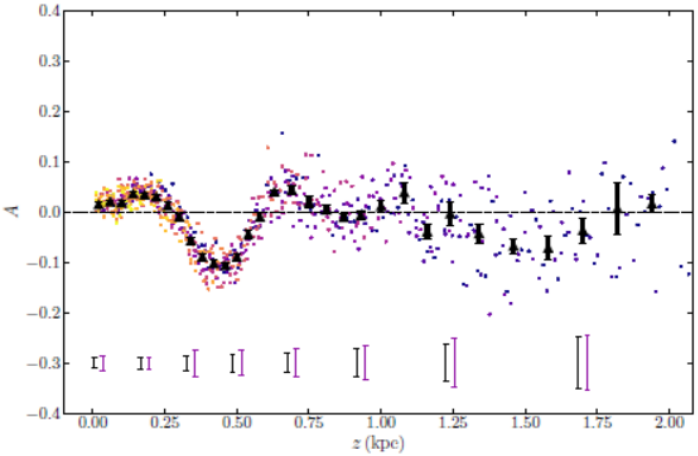

Fig.21 Asymmetry of the vertical number counts of the Milky Way shown as Fig.4 in Benett and Bovy (2018). Colors are assigned according to the stars' colors. Black triangles and error bars are calculated as median of different color bins by bootstrapping.

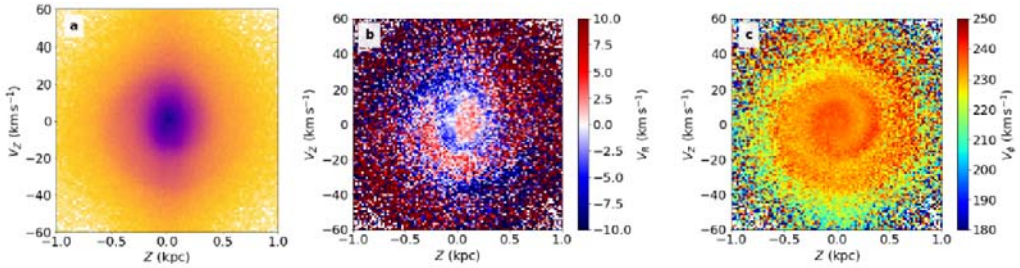

Figure 2. Distribution of stars in the vertical position-velocity plane Z-V_Z for stars selected as in Fig. 1. a) Two-dimensional histogram in bins of $\Delta Z = 0.01$ kpc and $\Delta V_Z = 0.1$ km s^{-1}; b) Z-V_Z plane coloured as a function of median V_R in bins of $\Delta Z = 0.02$ kpc and $\Delta V_Z = 1$ km s^{-1}; c) Same as b) but for V_ϕ.

Fig.22 Number counts, v_r and v_ϕ spirals in z-vz phase space shown as Fig.2 in Antoja et al (2018).

Reference:

Constance Rockosi et al, SEGUE-2 and APOGEE: Revealing the History of the Milky Way, 2009, ApJ, arXiv: 0902.3484

Gaia collaboration A.G.A.Brown et al, Gaia Data Release 2 Summary of the contents and survey properties, 2018, A&A 616, A1

Gaia Collaboration, C. Babusiaux et al, 2018, Gaia Data Release 2: Observational Hertzsprung-Russell diagrams, A&A, No.DR2HRD

Ackerman, A.S. & Marley, M.S., 2001, Precipitating Condensation Clouds in Substellar Atmospheres, AJ, 556, 87

Marley, M.S. et al, 2002, Clouds and Chemistry: Ultracool Dwarf Atmospheric Properties from Optical and Infrared Colors, arxiv: astro-ph/0105438v2

Lodders, K., 1999, Alkali Element Chemistry in Cool Dwarf Atmospheres, AJ, 519, 793

Allard.F et al, 2012a, Models of Stars, Brown Dwarfs and Exoplanets, A&A, 12a, Roy. Soc. London Philos. Trans.Ser. A, 370, 2765

Girardi L., 1999, A Secondary Clump of Red Giant Stars: Why and Where, MNRAS, 308, 818

Bergeron P. et al, 2011, A Comprehensive Spectroscopic Analysis Of Db White Dwarfs, ApJ, 737, 28

P.E.Tremblay et al, 2011, Solution to the problem of the surface gravity distribution of cool DA white dwarfs from improved 3D model atmospheres, A&A, 531, L19

Kleinman, S. J., Kepler, S. O., Koester, D., et al. 2013, ApJS, 204, 5

Paola M. et al, 2017, A New Generation of Parsec-Colibri Stellar Isochrones Including the Tp-Agb Phase, AJ, 835, 77

Mucciarelli A. et al, 2016, NGC6362: the least massive globular cluster with chemically distinct multiple populations, ApJ, 824, 73

Gaia collaboration, L.Eyer et al, 2018, Gaia Data Release 2: Variable stars in the color-absolute magnitude diagram, arXiv:1804.09382.

L.Eyer and J.Cuypers, 2000, Predictions on the number of variable stars for the GAIA space mission and for surveys as the ground-based International Liquid Mirror Telescope, ASP Conference Series, Vol. N

M.Benett and J.Bovy, 2018, Vertical waves in the Solar Neighborhood in Gaia DR2, MNRAS 000,1-9

L.Widrow et al, 2012, GALACTOSEISMOLOGY: DISCOVERY OF VERTICAL WAVES IN THE GALACTIC DISK, AJL, 750, L41

Antoja et al, Wrinkles in the Gaia data unveil a dynamically young and perturbed Milky Way disk, 2018, arXiv:1804.10196